

# Silicon optical diode with 40 dB nonreciprocal transmission

Li Fan,\* Leo T. Varghese, Jian Wang, Yi Xuan, Andrew M. Weiner, and Minghao Qi

Birck Nanotechnology Center and School of Electrical and Computer Engineering, Purdue University,  
West Lafayette, Indiana 47907, USA

\*Corresponding author: lfan@purdue.edu

Received January 23, 2013; revised February 28, 2013; accepted March 8, 2013;  
posted March 13, 2013 (Doc. ID 182747); published April 4, 2013

A passive all-silicon optical diode is demonstrated to realize a record high nonreciprocal transmission ratio (NTR) of 40 dB. Individual microrings that make up the device are experimentally studied to explain the nonlinear power dynamics. There is a compromise between the NTR and insertion loss, and possible solutions for further improvements are discussed. This work provides a way to realize extremely high optical nonreciprocity on chip for optical information processing applications. © 2013 Optical Society of America

OCIS codes: 230.5750, 230.3120.

Optical nonreciprocity (ONR) for on-chip information processing is highly desirable but has yet been elusive due to material and fabrication challenges. A number of ideas based on magneto-optic effect [1–5], indirect interband photonic transition [6,7], and electro-absorption modulation [8] have been investigated, with various levels of success and drawbacks. Recently we demonstrated a passive optical diode based on cascaded nonlinear microring resonators [9]. It does not require any externally applied fields and operates on the input light itself. It is based on silicon and is compatible with complementary metal-oxide-semiconductor processing.

The all-silicon optical diode (ASOD) uses the thermo-optic effect of silicon [10]. Although this nonlinearity is inherently slow, we have demonstrated packet switching of 10 Gb/s data with the ASOD [11]. Furthermore, faster nonlinearities could be accessed by suppressing the thermal effects, though at the cost of increased operating power [12]. The ASOD is different from the traditional optical isolators in that it is reciprocal when light is applied from both directions simultaneously. Nevertheless, the use of faster nonlinearities would allow the device to achieve one-way data transmission as long as sufficient time interval exists between individual optical pulses. In addition, the current ASOD architecture has been shown to function as an optical transistor, showing promise as a building block for optical signal processing [13]. In this Letter, we study the power dynamics of the microrings that make up the ASOD. We also report an optical diode with 40 dB ONR, 12 dB higher than our prior results [9] and 10 dB higher than the best chip-level ONR previously reported [8].

The device structure is shown in Fig. 1. It is made up of two 5  $\mu\text{m}$  radius silicon microring resonators: an asymmetrically coupled add-drop filter (ADF), and a notch filter (NF). The NF is coupled to the top bus waveguide with a gap  $G_1$  (400 nm). The ADF is coupled to the top and bottom bus waveguides with  $G_2$  (550 nm) and  $G_3$  (500 nm), respectively. These values are slightly different from our previous design in [9]. The device is fabricated on a 250 nm silicon-on-insulator platform with a waveguide width of 500 nm and a buried oxide of 3  $\mu\text{m}$ . A titanium microheater is placed to the side of the NF to thermally tune it to match the resonance of the ADF.

While no overcladding is used, SU8 resist is patterned over the vertical grating couplers to efficiently couple TM light in and out of the two ports with a fiber–chip–fiber loss of 13 dB at 1580 nm. All power values are calculated at the device, by assuming the input and output grating couplers have identical loss. The power loss suffered by light going through a device is defined as insertion loss, which does not include the fiber–chip–fiber loss. Light entering from Port I and exiting Port II is designated as forward direction while light entering Port II and exiting Port I is designated as backward direction. For the first part of this Letter, an ADF and NF are chosen from an ASOD with their resonance wavelengths slightly mismatched to study their power dependence separately without cross talk.

An NF, shown in Fig. 2(a), is a two-terminal device with a ring cavity coupled to a bus waveguide. Its transmission shows strong attenuations at resonance wavelengths, of which the optical length is an integer multiple. The transmission spectra of the NF for a wide range of input powers are shown in Fig. 2(b). At low powers, the dip is symmetric, indicating that the microring is working in the linear regime. With the operating wavelength chosen as the dip wavelength at lowest input power, the insertion loss shown in Fig. 2(c) is constant at  $\sim 22$  dB, which is the extinction ratio of this particular microring. As the power increases, the resonance dip redshifts due to the onset of nonlinearity through the thermo-optic effect of silicon [14]. When the input power increases beyond  $-15$  dBm, light at the operating wavelength is no longer coupled well into the cavity, resulting in it passing directly to the output (throughport), leading to a decreasing insertion loss, shown in Fig. 2(c). The insertion loss starts to reduce and sinks below 1.6 dB at an

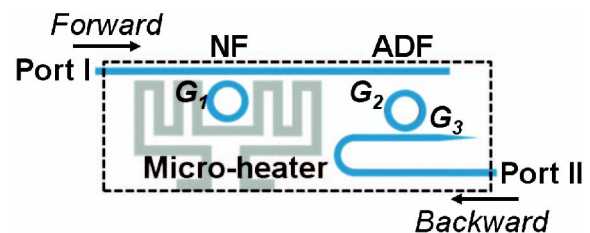


Fig. 1. Schematic diagram of the ASOD.

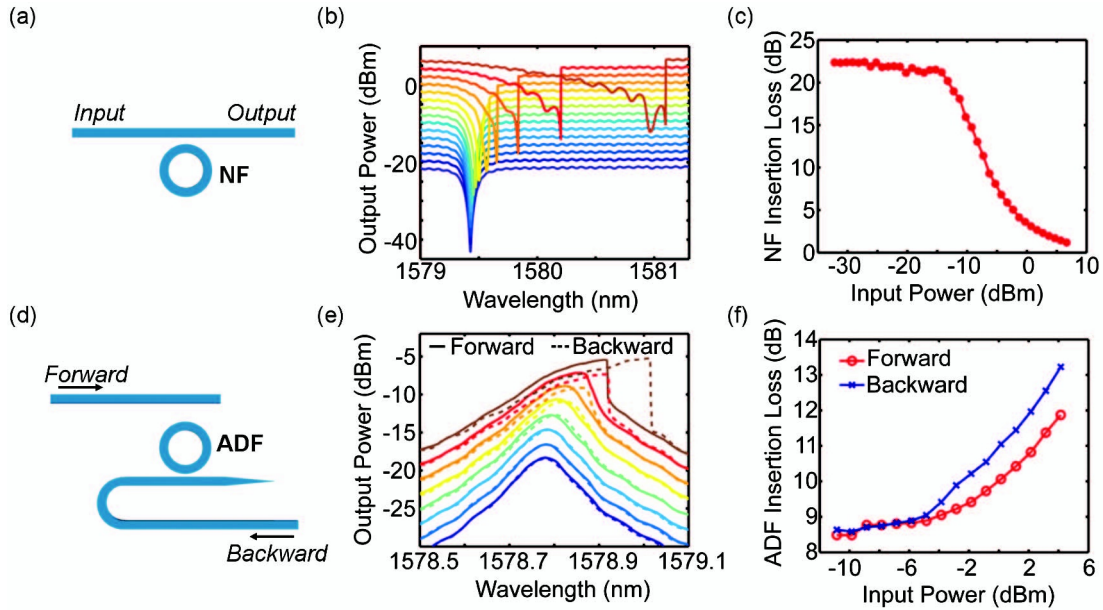


Fig. 2. Power dynamics of the NF and ADF. (a) Schematic of the NF. (b) Transmission spectra of the NF for input power varied from  $-21.3$  dBm to  $6.7$  dBm in steps of  $2$  dB. (c) Insertion loss of the NF as a function of the input power at  $1579.43$  nm. (d) Schematic of the ADF. (e) Transmission spectra of the ADF for input powers varied from  $-10.9$  dBm to  $4.2$  dBm in steps of  $2$  dB. (f) Insertion loss of the ADF in the forward and backward directions as a function of the input power at  $1578.78$  nm.

input power beyond  $5$  dBm. Hence, the NF provides high insertion loss at low input power and low insertion loss at high input power.

For an ADF, shown in Fig. 2(d), it is a four-terminal device with a ring cavity coupled to two bus waveguides asymmetrically. The transmission spectra at different input powers for the forward and backward directions are plotted in Fig. 2(e). At low powers, the ADF stays in the linear regime, resulting in identical spectra for both the forward and backward directions. Choosing this peak as the operating wavelength, the insertion loss, also called drop loss, of the ADF remains constant at low powers, as shown in Fig. 2(f). At input powers above  $-5$  dBm, the insertion loss for both directions starts to increase in a similar trend, indicating the onset of nonlinearity, with the backward direction suffering higher insertion loss than the forward. The increase in insertion loss is because a higher percentage of the light at the operating wavelength is not coupled into the cavity, resulting in a decreasing transmission at the drop port. Once nonlinearity has set in, increasing input power redshifts the backward peak faster than the forward. This is because higher energy is accumulated in the microring when light enters from the stronger coupling side. As the input power further increases, both directions continue to suffer higher and higher insertion loss, suggesting the output power undergoes saturation.

From this, the operation of the ASOD can be explained as follows. Assume the NF and ADF have the same operating wavelength (this can be practically realized through thermal tuning). In the forward direction, a high input power passes the NF with low insertion loss, and is dropped across the ADF to provide a high transmission, albeit suffering an insertion loss. In the backward direction, light first suffers a high insertion loss across the ADF, which then reaches the NF at a relatively low power. At the NF, it suffers another significant insertion

loss, thereby creating a low transmission. The contrast between the forward and backward transmission is defined as the nonreciprocal transmission ratio (NTR), an important criterion to evaluate how efficiently the diode can provide one-way transmission.

Several key points can be drawn from this study. First, the NF is the main contributor to NTR. To obtain high NTR, the NF needs to have the maximum extinction ratio, which can be achieved by operating the microring at critical coupling. Second, the ADF's asymmetric architecture also contributes to the NTR, but to a lesser extent. While the insertion loss of the ADF initiates ONR, its saturation effect allows the ASOD to maintain high NTR at high powers. This differentiates the function of ADF from a simple constant-loss mechanism, which would break down at high backward powers. Third, to maximize the ONR effect, in the forward direction the input power

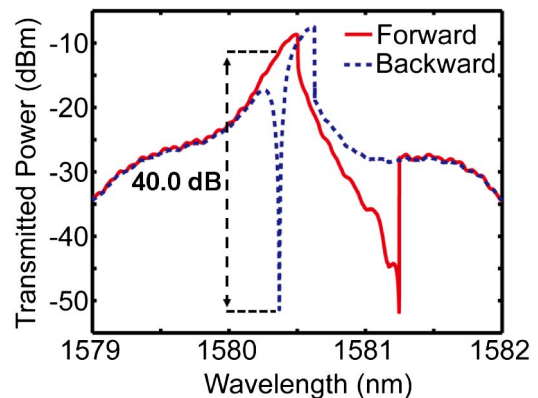


Fig. 3. (Color online) Transmission spectra of forward and backward transmission of the ASOD at an input power of  $3.55$  dBm ( $\sim 2.3$  mW). An NTR of  $40.0$  dB is observed. Note that this is a different ASOD device from the one used in Fig. 2.

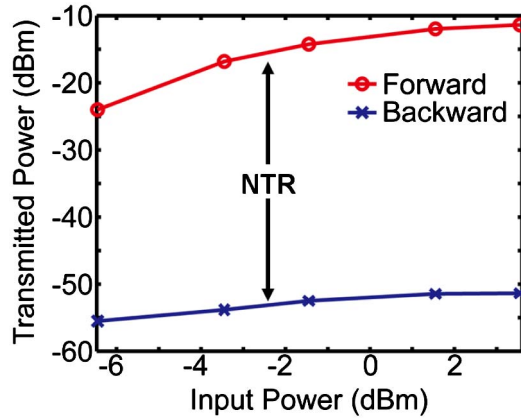


Fig. 4. (Color online) ASOD's forward and backward transmitted power versus input power. NTR (dB) = forward transmitted power (dBm) – backward transmitted power (dBm). Insertion loss = input power – forward transmitted power.

needs to be high enough so that NF has minimum insertion loss, while in the backward direction the input power needs to be low enough to ensure that NF works in the linear regime. This large input power difference is required and provided by the ADF's insertion loss, which becomes the major part of the insertion loss of the whole device. So, the key to reducing the device insertion loss while maintaining high NTR lies in having a sharper slope in Fig. 2(c). This could be achieved by having an NF with a high quality factor or using stronger nonlinearities through a different material platform.

By scanning multiple ASOD devices with the same parameters, we chose a device with an NF having the largest extinction and with resonance extremely close to the ADF's resonance. Figure 3 shows the transmission spectra of this ASOD, realizing an NTR of 40 dB at  $\sim 2.3$  mW, the highest ever reported on-chip, to the best of our knowledge. Figure 4 plots the transmitted power for the forward and backward directions at various input powers. For input powers higher than 230  $\mu$ W, NTR is higher than 30 dB. At 40 dB NTR, the insertion loss is 15.5 dB, obtained by subtracting the forward transmitted power from the input in Fig. 4. Table 1 presents the results of recent on-chip experimental demonstrations of high ONR devices. In most works, a high NTR also comes with a high insertion loss. Methods to reduce the insertion loss while maintaining high NTR have become critical for any realistic device level integration.

In conclusion, we study the power dynamics of the individual microrings in an optical diode. The results help to explain the mechanism of the optical diode and provide insights for further device optimization. We report an NTR of 40 dB, the highest ever reported on-chip, to the best of our knowledge. This Letter provides an

**Table 1. NTR and Insertion Loss of Recent Experimental Demonstrations of On-Chip ONR**

References	NTR (dB)	Insertion Loss (dB)
[7]	3	70
[2]	$19.5 \pm 2.9$	$18.8 \pm 1.1$
[5]	21	8
[9]	28	12
[8]	30	23.8
This work	40	15.5

experimental exploration of the key nonlinear phenomena for devices such as optical diodes and optical transistors [13] based on microring resonators.

This work is supported by Air Force Office of Scientific Research grant FA9550-08-1-0379, National Science Foundation grants ECCS-0925759, ECCS-0901383 and CNS-1126688, and National Institutes of Health grant 1R01RR026273-01. M. Q. acknowledges partial support from CAS International Collaboration and Innovation Program on High Mobility Materials Engineering.

## References

1. R. L. Espinola, T. Izuhara, M. C. Tsai, R. M. Osgood, and H. Dotsch, *Opt. Lett.* **29**, 941 (2004).
2. L. Bi, J. J. Hu, P. Jiang, D. H. Kim, G. F. Dionne, L. C. Kimerling, and C. A. Ross, *Nat. Photonics* **5**, 758 (2011).
3. T. R. Zaman, X. Guo, and R. J. Ram, *Appl. Phys. Lett.* **90**, 023514 (2007).
4. R. El-Ganainy, P. Kumar, and M. Levy, *Opt. Lett.* **38**, 61 (2013).
5. Y. Shoji, T. Mizumoto, H. Yokoi, I. W. Hsieh, and R. M. Osgood, *Appl. Phys. Lett.* **92**, 071117 (2008).
6. Z. Yu and S. Fan, *Nat. Photonics* **3**, 91 (2009).
7. H. Lira, Z. F. Yu, S. H. Fan, and M. Lipson, *Phys. Rev. Lett.* **109**, 033901 (2012).
8. S. K. Ibrahim, S. Bhandare, D. Sandel, H. Zhang, and R. Noe, *Electron. Lett.* **40**, 1293 (2004).
9. L. Fan, J. Wang, L. T. Varghese, H. Shen, B. Niu, Y. Xuan, A. M. Weiner, and M. Qi, *Science* **335**, 447 (2012).
10. J. Wang, L. Fan, L. T. Varghese, H. Shen, Y. Xuan, B. Niu, and M. Qi, *J. Lightwave Technol.* **31**, 313 (2013).
11. J. Wang, L. Fan, L. T. Varghese, F. Gan, X. Wang, J. C. Wirth, B. Niu, Y. Xuan, D. E. Leaird, A. M. Weiner, and M. Qi, in *IEEE Photonics Conference (IPC)* (IEEE, 2012), pp. 703–704.
12. K. Nozaki, A. Shinya, S. Matsuo, Y. Suzuki, T. Segawa, T. Sato, Y. Kawaguchi, R. Takahashi, and M. Notomi, *Nat. Photonics* **6**, 248 (2012).
13. L. T. Varghese, L. Fan, J. Wang, F. Gan, X. Wang, J. Wirth, B. Niu, C. Tansarawiput, Y. Xuan, A. M. Weiner, and M. Qi, in *Frontiers in Optics Conference*, OSA Technical Digest (online) (Optical Society of America, 2012), paper FW6C.6.
14. G. Cocorullo and I. Rendina, *Electron. Lett.* **28**, 83 (1992).